Since January 2020 Elsevier has created a COVID-19 resource centre with free information in English and Mandarin on the novel coronavirus COVID-19. The COVID-19 resource centre is hosted on Elsevier Connect, the company's public news and information website.

Infection, Genetics and Evolution 85 (2020) 104439

Contents lists available at ScienceDirect

Infection, Genetics and Evolution

journal homepage: www.elsevier.com/locate/meegid

Short communication

Bioinformatics analysis reveals four major hexon variants of human adenovirus type-3 (HAdV-3) as the potential strains for development of vaccine and siRNA-based therapeutics against HAdV-3 respiratory infections

Somnath Panda[a,*], Urmila Banik[b], Arun K. Adhikary[a]

[a] Unit of Microbiology, AIMST University, Faculty of Medicine, Jalan Bedong Semeling, 08100 Bedong, Kedah, Malaysia
[b] Unit of Pathology, AIMST University, Faculty of Medicine, Jalan Bedong Semeling, 08100 Bedong, Kedah, Malaysia

ARTICLE INFO

Keywords:
Human adenovirus type 3
Respiratory infections
Hexon variants
Vaccine
siRNA

ABSTRACT

Human adenovirus type 3 (HAdV-3) encompasses 15–87% of all adenoviral respiratory infections. The significant morbidity and mortality, especially among the neonates and immunosuppressed patients, demand the need for a vaccine or a targeted antiviral against this type. However, due to the existence of multiple hexon variants (3Hv-1 to 3Hv-25), the selection of vaccine strains of HAdV-3 is challenging. This study was designed to evaluate HAdV-3 hexon variants for the selection of potential vaccine candidates and the use of hexon gene as a target for designing siRNA that can be used as a therapy. Based on the data of worldwide distribution, duration of circulation, co-circulation and their percentage among all the variants, 3Hv-1 to 3Hv-4 were categorized as the major hexon variants. Phylogenetic analysis and the percentage of homology in the hypervariable regions followed by multi-sequence alignment, zPicture analysis and restriction enzyme analysis were carried out. In the phylogram, the variants were arranged in different clusters. The HVR encoding regions of hexon of 3Hv-1 to 3Hv-4 showed 16 point mutations resulting in 12 amino acids substitutions. The homology in HVRs was 81.81–100%. Therefore, the major hexon variants are substantially different from each other which justifies their inclusion as the potential vaccine candidates. Interestingly, despite the significant differences in the DNA sequence, there were many conserved areas in the HVRs, and we have designed functional siRNAs form those locations. We have also designed immunogenic vaccine peptide epitopes from the hexon protein using bioinformatics prediction tool. We hope that our developed siRNAs and immunogenic vaccine peptide epitopes could be used in the future development of siRNA-based therapy and designing a vaccine against HAdV-3.

Human adenovirus type 3 (HAdV-3) is accountable for 15 to 87% of all adenoviral respiratory infections worldwide with severe morbidity (Kenmoe et al., 2018; Lin et al., 2019; Lynch and Kajon, 2016). Moreover, some strains of HAdV-3 are responsible for 3.6 to 50% fatality among the paediatric age group (Adhikary, 2017; Kajon et al., 1990; Kim et al., 2003; Lai et al., 2013). Therefore, development of a vaccine or a targeted therapy against HAdV-3 is in demand considering its clinical significance.

Hexon protein forms major portion of the HAdV capsid (Russell, 2009). The neutralizing epitopes are located in one or more of the seven hypervariable regions (HVRs) of the hexon (Crawford-Miksza and Schnurr, 1996; Pichla-Gollon, n.d.). Therefore, analysis of HVRs of hexon is extremely important for vaccine strain selection. The worldwide circulating strains of HAdV-3 are categorized into 25 hexon variants (3Hv-1 to 3Hv-25) based on the heterogeneity of the HVRs (Haque et al., 2018), which makes the selection of vaccine strain complicated.

So far, there is no targeted and clinically proven anti-adenoviral, although nucleoside analogues and protease inhibitors showed limited activity (Lion, 2014; Matthes-Martin et al., 2013; Wold et al., 2019). In this regard, synthetic oligonucleotide-based RNA interference (RNAi) provides a tremendous opportunity for the development of oligonucleotide-based drugs (Ge et al., 2003). Among them, small interfering RNAs (siRNAs) has been used as therapeutics against a number of human pathogenic viruses (Ge et al., 2004; Hamasaki et al., 2003; Moore et al., 2005; Zender et al., 2003).

In this study, we have analysed all the hexon variants of HAdV-3 based on various criteria, followed by the molecular analysis of their HVRs to assess their appropriateness as potential vaccine candidates. Then, we have identified the conserved locations in HVR encoding regions of the hexon gene and from those locations we have designed functional siRNAs. Next, we have also designed immunogenic vaccine peptide epitopes from the hexon protein that can be used to design a

* Corresponding author at: Unit of Microbiology, AIMST University, Faculty of Medicine, 08100, Bedong, Kedah Darul Aman, Malaysia.
E-mail address: somnathpanda86@yahoo.co.uk (S. Panda).

https://doi.org/10.1016/j.meegid.2020.104439
Received 7 January 2020; Received in revised form 24 April 2020; Accepted 20 June 2020
Available online 23 June 2020

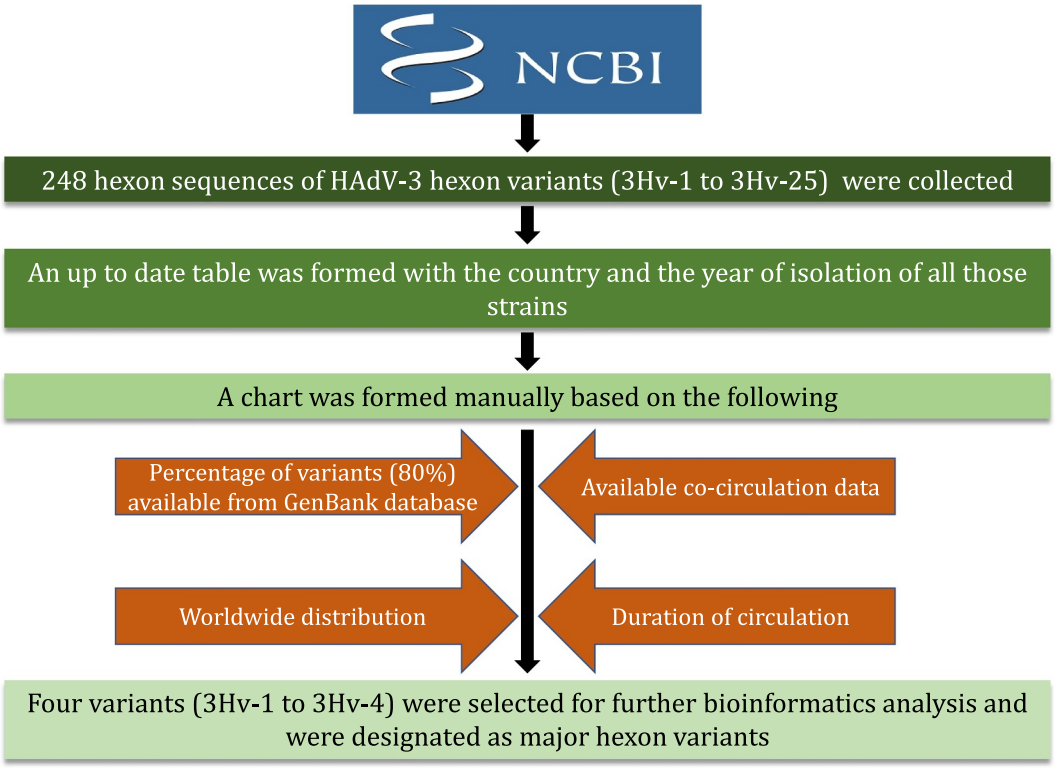

Fig. 1. Initial steps for the selection of four hexon variants of HAdV-3. The AA sequences that include the seven HVRs of the GB strain (GenBank accession no. AB330084) and the available 248 field strains of HAdV-3 hexon variants (3Hv-1 to 3Hv-25) were collected from "NCBI" (http://www.ncbi.nlm.nih.gov/). Several criteria (the percentage among the variants, the available co-circulation data, their distribution among different countries and the duration of their circulation) were considered for the selection of vaccine strains. Based on those criteria, four hexon variants (3Hv-1 to 3Hv-4) were selected for further bioinformatics analysis.

vaccine. We anticipate that our developed siRNAs and peptide epitopes could be used in the development of siRNA-based therapy and designing a future vaccine against HAdV-3.

The amino acid (AA) sequences that include the seven HVRs of 25 hexon variants and prototype strain (GB-GenBank accession no. AB330084) were collected from NCBI (http://www.ncbi.nlm.nih.gov/). Hexon variants were selected based on their duration of circulation, co-circulation and worldwide distribution. The selection process is depicted in Fig. 1.

To explore the variations, the 319 AA long sequence (extending from 132 to 450) that included the seven HVRs of the GB strain and 3Hv-1 to 3Hv-4 were aligned by Genetyx software (www.genetyx.co.jp). After alignment the number of AA variations in all the HVRs was observed. Then the differences in AA sequences in all the HVRs were tabulated and the percentage of homologies were calculated manually as compared to the GB strain.

A phylogenetic tree was constructed with the help of the Phylogeny.fr website (http://www.phylogeny.fr/documentation.cgi) (Dereeper et al., 2008) using the "One Click mode". It has been designed to provide a high-performance platform that transparently chains programs relevant to phylogenetic analysis in a comprehensive and flexible pipeline. By default, the pipeline is already set up to run and connect programs recognized for their accuracy and speed (MUSCLE for multiple alignment and PhyML for phylogeny) to reconstruct a robust phylogenetic tree. The 319AA long (extending from 132 to 450) sequence of 25 hexon variants (3Hv-1 to 3Hv-25) and GB strain were uploaded to the website in FASTA format to build the phylogram.

The variations among the HVR encoding regions of the hexon gene of 3Hv-1 to 3Hv-4 were shown by multi-sequence alignment (MSA), in silico RE analysis (http://rebase.neb.com/rebase/rebase.html) and zPicture analysis (http://zpicture.dcode.org/) (Ovcharenko et al., 2004).

For MSA, the 957 bp long (encoding the 7 HVRs) nucleotide (NT) sequences that extend from 394 bp to 1350 bp of the hexon gene of the GB strain and 3Hv-1 to 3Hv-4 hexon variants were collected from the database of "NCBI" and were aligned using Genetyx software to find out the conserved regions as well as the variation. After identifying the conserved regions, we also aligned the other 21 variants (3Hv-5 to 3Hv-25) to examine whether those same conserved regions exist among the rest of the variants. However, only the alignment data of the GB strain and 3Hv-1 to 3Hv-4 has been shown here as they are the principal variants for analysis in this study. The total number of NT variations on the HVRs among 3Hv-1 to 3Hv-4 were counted manually after the alignment.

In silico RE digestions were performed with *Bcc*I, *Bco*DI, *Bsp*1286I and *Bst*NI. From the New England Biolab website, REBASE tools were

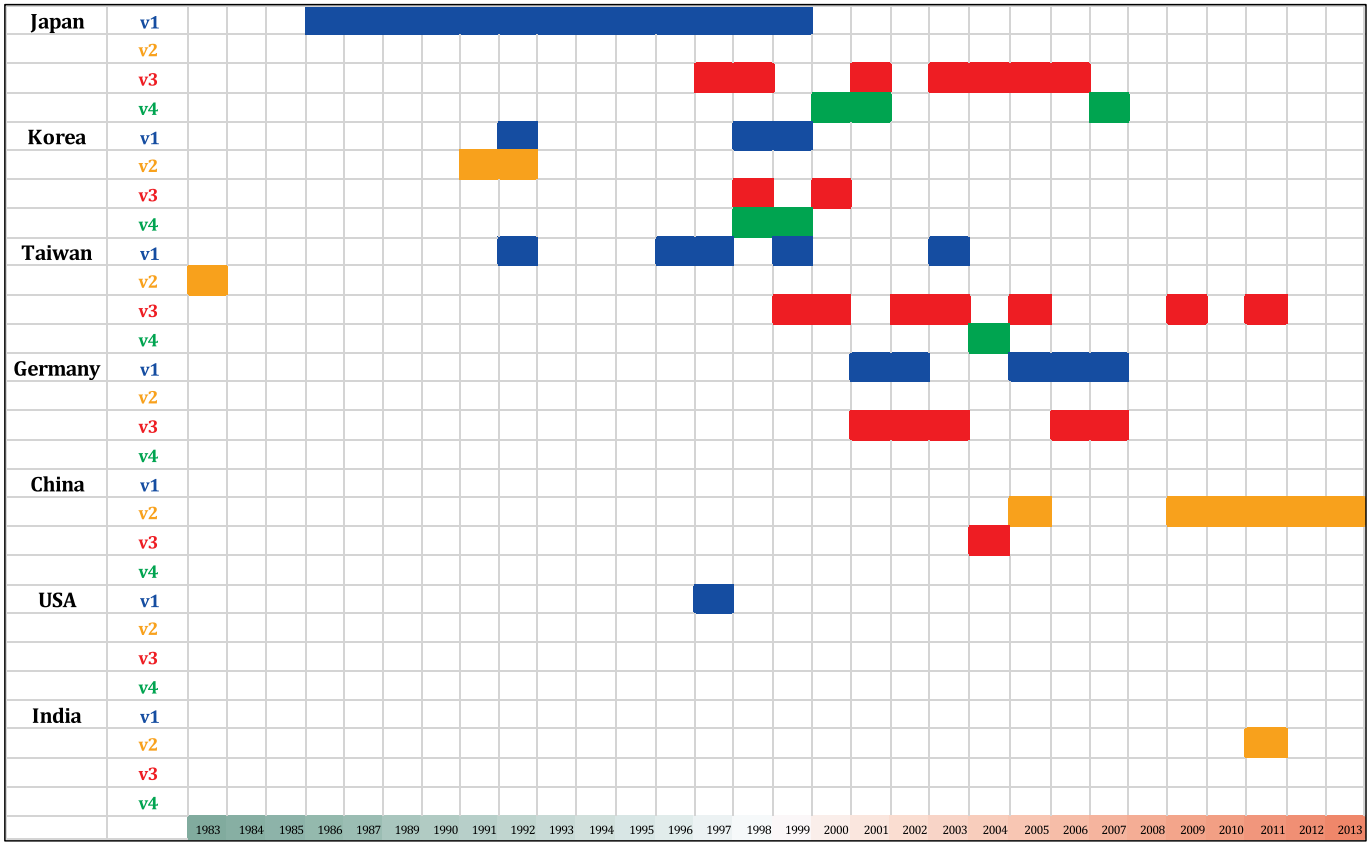

Fig. 2. The circulation and co-circulation of four major hexon variants (3Hv-1 to 3Hv-4) based on the available data among seven countries until 2013. 3Hv-1, 3Hv-2, 3Hv-3 and 3Hv-4 were depicted in blue, orange, red and green respectively. We found that the co-circulation of the four major hexon variants was highly prevalent in Korea followed by Germany among those seven countries. In Korea, 3Hv-1 and 2 co-circulated in 1992, and 3Hv-1, 3 and 4 in 1998. 3Hv-1 and 4 again co-circulated in 1999. A single hexon variant also circulated among different countries in the same year, such as 3Hv-1 in Japan, Korea and Taiwan in 1992, and 3Hv-3 in Japan and Germany in 2001. (For interpretation of the references to colour in this figure legend, the reader is referred to the web version of this article.)

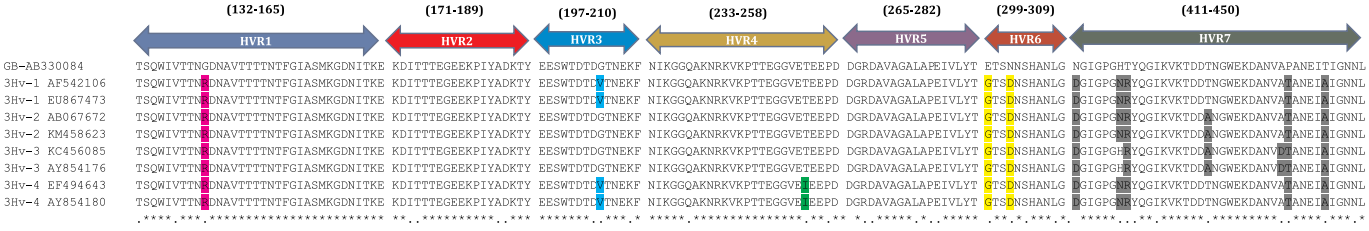

Fig. 3. Comparison of the AA sequences of seven HVRs of hexon of GB strain and 4 major hexon variants (3Hv-1 to 3Hv-4). The AA sequences of the seven HVRs of GB strain and 3Hv-1 to 3Hv-4 were aligned by Genetyx software. The intervening regions were deleted after alignment. The AA variations as compared to the GB strain at different position of HVRs are indicated by a dot (.) at the bottom and the homologies are represented with an asterisk (*). There were no variations in two HVRs (HVR2 and 5) when compared to the GB sequence. The variations among the rest of the HVRs (HVR1, 3, 4, 6 and 7) in comparison to GB are indicated by highlighting in different colours. The locations of the HVRs in the hexon protein are mentioned in brackets on top.

selected. From the REBASE tools icon, theoretical digest with all the REBASE prototypes icon was selected and opened. Then 957 bp long hexon nucleotide sequences that extend from 394 bp to 1350 bp of the GB strain along with 3Hv-1 to 3Hv-4 were individually pasted in FASTA format for digestion with 1.2% agarose. After digestion, the individual enzyme was selected and the restriction patterns were saved. The 100 bp molecular weight marker (M) was used to detect the molecular weight of the DNA fragments. Then, the restriction profile of *Bcc*I, *Bco*DI, *Bsp*1286I and *Bst*NI for all the stains were manually arranged side by side for comparison.

Table 1
Variations of amino acid (AA) sequences in the HVRs of hexon of 3Hv-1 to 3Hv-4.

Variant	HVR-1 (132–165)	HVR-2 (171–189)	HVR-3 (197–210)	HVR-4 (233–258)	HVR-5 (265–282)	HVR-6 (299–309)	HVR-7 (411–450)
3Hv-1	141st AA R(G)	No Variations	205th AA V(G)	No Variations	No Variations	299th AA G(E) 302nd AA D(N)	411th AA D(N) 417th AA N(H) 418th AA R(T) 429th AA A(T) 440th AA T(P) 445th AA A(T)
3Hv-2	141st AA R(G)	No Variations	No Variations	No Variations	No Variations	299th AA G(E) 302nd AA D(N)	411th AA D(N) 417th AA N(H) 418th AA R(T) 429th AA A(T) 440th AA T(P) 445th AA A(T)
3Hv-3	141st AA R(G)	No Variations	No Variations	No Variations	No Variations	299th AA G(E) 302nd AA D(N)	411th AA D(N) 418th AA R(T) 429th AA A(T) 439th AA D(A) 440th AA T(P) 445th AA A(T)
3Hv-4	141st AA R(G)	No Variations	205th AA V(G)	254th AA I(T)	No Variations	299th AA G(E) 302nd AA D(N)	411th AA D(N) 417th AA N(H) 418th AA R(T) 440th AA T(P) 445th AA A(T)

The numbers inside the parentheses in the top row indicate the locations of the HVRs based on the AA sequence of the GB strain. Inside the table, the numbers signify the positions of the AA substitutions and the highlighted letter indicates the name of the AA in an abbreviated form that has substituted the AA present in the GB sequence (as mentioned within brackets).

Table 2
The percentage of AA homologies in the 7 HVRs of the four major hexon variants of HAdV-3 as compared to the GB strain.

Variant	Country	HVR-1	HVR-2	HVR-3	HVR-4	HVR-5	HVR-6	HVR-7
3Hv-1 (AF542106)	Korea	97.05	100	92.85	100	100	81.81	87.50
3Hv-1 (EU867473)	Germany	97.05	100	92.85	100	100	81.81	87.50
3Hv-1 (AB067662)	Japan	97.05	100	92.85	100	100	81.81	87.50
3Hv-2 (KM458623)	Korea	97.05	100	100	100	100	81.81	85
3Hv-2 (AB067672)	Japan	97.05	100	100	100	100	81.81	85
3Hv-2 (KF268210)	India	97.05	100	100	100	100	81.81	85
3Hv-3 (KC456085)	Taiwan	97.05	100	100	100	100	81.81	85
3Hv-3 (AB366423)	Japan	97.05	100	100	100	100	81.81	85
3Hv-3 (AY854176)	Korea	97.05	100	100	100	100	81.81	85
3Hv-4 (AY854180)	Korea	97.05	100	92.85	96.15	100	81.81	87.50
3Hv-4 (AB366417)	Japan	97.05	100	92.85	96.15	100	81.81	87.50
3Hv-4 (EF494643)	Taiwan	97.05	100	92.85	96.15	100	81.81	87.50

The GenBank accession nos. are mentioned in the parentheses of each selected hexon variant.

A comparative study of the HVR encoding regions of the hexon gene of the four HAdV-3 major hexon variants (3Hv-1 to 3Hv-4) with the GB strain was conducted using the zPicture dynamic alignment and visualization tool. For this, the multi-picture option was selected from the website and the 957 bp hexon nucleotide sequences that extend from 394 bp to 1350 bp of HAdV-3 GB strain and 3Hv-1 to 3Hv-4 were uploaded in FASTA format. zPicture compares the nucleotide sequences of pairs of genomes using a moving overlapping window and scoring percent identities. The 'x' axis is the size of the nucleotide sequence in kilobases and the 'y' axis is the percent identity. The 'y' axis was set between 90% and 100%, indicating a very high level of identity. The gapless display blocks indicate homology and the intervening gap regions indicate a lack of homology.

Numerous tools are available to design functional siRNAs such as MysiRNA-designer (Mysara et al., 2011), siDirect (Naito et al., 2009) and siMAX-siRNA Designer (https://eurofinsgenomics.eu/en/dna-rna-

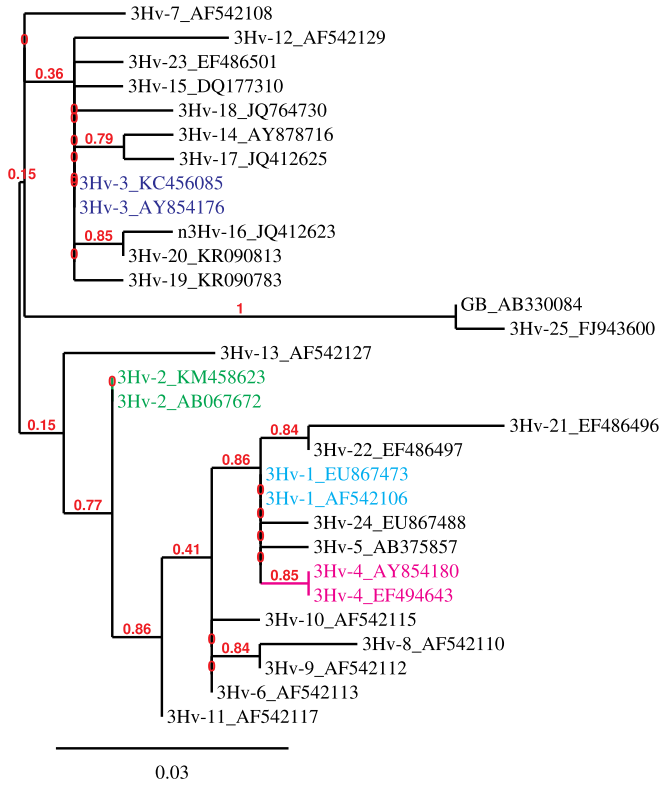

Fig. 4. Phylogenetic analysis of the partial hexon polypeptide of different hexon variants of HAdV-3. Two strains of 3Hv-1 to 3Hv-4 and one from the rest of the 25 variants were used for this analysis. The hexon variants (3Hv-1 to 3Hv-25) were segregated into multiple clusters. Two of the four major hexon variants (3Hv-1 and 3Hv-4) were included in the same cluster. However, 3Hv-2 and 3Hv-3 were included in different clusters.

oligonucleotides/custom-dna-rna-oligos/simax-sirna/) etc. In this study, siDirect 2.0 (http://sidirect2.rnai.jp) has been used to design functional siRNAs from the conserved regions found in all hexon variants (3Hv-1 to 3Hv-25). siDirect 2.0 algorithm eliminates off-target effects by reflecting the recent finding that the capability of siRNA to induce off-target effect is highly correlated to the thermodynamic stability, or the melting temperature (Tm), of the seed-target duplex. Hence, the selection of siRNAs with lower seed-target duplex stabilities (benchmark Tm < 21.5 °C) minimizes the off-target effects. It generates and filters siRNAs in three selection steps: step 1 involves the selection of highly functional siRNAs, step 2 involves the reduction of seed-dependent off-target effects and step 3 involves the elimination of near-perfect matched genes (Fookolaee et al., 2019).

We used NetMHC 4.0 (http://www.cbs.dtu.dk/services/NetMHC/) to predict MHC class I binding epitopes. For this, the 319 AA long sequences (extending from 132 to 450) that included the seven HVRs of 3Hv-1 to 3Hv-4 were uploaded in FASTA format. We chose 9mer peptides as most HLA molecules have a strong preference for binding to 9mer peptides. The peptides were identified as a strong binder if the % rank is below the specified threshold for the strong binders, by default 0.5%. On the other hand, the peptide was identified as a weak binder if the % rank is above the threshold of the strong binders but below the specified threshold for the weak binders, by default 2%.

Among the 25 hexon variants, 3Hv-1 to 3Hv-4 comprised 80% of all the variants. We found that they are most prevalent in 7 countries (Japan, Korea, Taiwan, Germany, China, USA and India) as depicted in Fig. 2. Hence, considering the percentage among the variants, global distribution and duration of circulation, we considered 3Hv-1 to 3Hv-4 as the major hexon variants.

The alignment data showed remarkable AA sequence variations among the HVRs of 3Hv-1 to 3Hv-4 as compared to the GB strain. The highest number of 7 variations was found in HVR7 followed by 2 variations in HVR6 (Fig. 3). The locations of the AA substitutions are shown in Table 1. The lowest percentage of homology (81.81%) was found in HVR6 of all the variants. In the remaining HVRs (HVR1, 2, 3, 4, 5 and 7), the percentage of homologies were calculated as 97.05%, 100%, 92.85 to 100%, 96.15 to 100%, 100%, and 85 to 87.5% respectively (Table 2).

The different hexon variants (3Hv-1 to 3Hv-25) were segregated into multiple clusters in the phylogenetic tree as shown in Fig. 4. Two of the four major hexon variants (3Hv-1 and 3Hv-4) were incorporated in the same cluster. However, 3Hv-2 and 3Hv-3 were included in a different cluster. Multiple major clusters are formed due to their heterogeneity of the AA sequence in the HVRs.

The NT alignment data of the GB strain and the four major hexon variants of HAdV-3 (3Hv-1 to 3Hv-4) showed a total number of 16 point mutation on the seven HVRs (Fig. 5). There are substantial numbers of conserved regions within the variation in the gene which are depicted in Table 3. The rest of the variants (3Hv-5 to 3Hv-25) also showed similar conserved regions.

In silico DNA restriction patterns with restriction endonuclease *Bcc*I, *Bco*DI, *Bsp*1286I and *Bst*NI clearly differentiated GB from 3Hv-1 to 3Hv-4 (Fig. 6A). Similarly, the zPicture analysis also clearly depicted the variations (Fig. 6B).

We found 10 conserved regions in the HVR encoding portion among all HAdV-3 hexon variants as presented in Table 3. For example, the functional siRNAs designed from the first sequence is shown in Fig. 7. The functional siRNAs designed from the other conserved regions are also shown in the supplementary data 1. However, we could not obtain any functional siRNAs from the conserved region numbers 4 and 6 when the seed-duplex stability (T_m) was < 21.5 °C. We did not try to design functional siRNAs by relaxing the parameters as T_m < 21.5 °C is the minimum requirement for getting off-target reduced functional siRNAs.

MHC class I binding epitopes of 9mer peptides were predicted from NetMHC 4.0. All HLA-A alleles were selected for this. A total number of 311 epitopes were predicted for HLA-A0101. Among them there were 2 strong binders and 5 weak binders based on their %rank as shown in Table 4. The complete dataset of MHC class I binding epitopes prediction from 3Hv-1 has been shown in the supplementary data 2.

HAdV-3 respiratory infections have become a global concern, especially among Asian countries (Zou et al., 2012). The only

Fig. 5. The NT alignment data of the GB strain and the four major hexon variants of HAdV-3 (3Hv-1 to 3Hv-4) (GenBank accession nos. AB330084, AF542106, AB067672, KC456085 and AY854180). The total number of variations on the seven HVRs were 16. No variations were found on the encoding regions of HVR2 and HVR5. The NT variations as compared to the GB strain at different position of HVRs are indicated by a dot (.) at the bottom and the homologies are represented with an asterisk (*). Genetyx software was used for the alignment. The encoding regions of the seven HVRs were highlighted in seven different colours and their positions on the hexon gene were mentioned within the brackets.

Table 3
Conserved regions in the HVR encoding portion among all HAdV-3 hexon variants.

Number	Positions in hexon gene (GB strain) *	Sequence
1.	424 bp - 516 bp	GACAATGCAGTAACTACCACCACAAACACATTTGGCATTGCTTCCATGAAGGGAGACAATATTACTAAAGAAGGTTTGCAAATTGGGAAAGAC
2.	518 bp - 555 bp	TTACCACTACTGAAGGAGAAGAAAAGCCCATTTATGCC
3.	571 bp - 613 bp	CCAGAGCCTCAAGTTGGAGAAGAATCATGGACTGATACTGATG
4.	634 bp - 710 bp	GGAAGAGCCCTTAAACCAGCTACCAACATGAAGCCATGCTACGGGTCTTTTGCAAGACCTACAAACATAAAAGGGGG
5.	714 bp - 740 bp	AGCTAAAAACAGAAAAGTAAAACCAAC
6.	778 bp - 800 bp	GATATGGAATTTTTCGATGGTAG
7.	983 bp - 1039 bp	GCCTAATGTACTACAACAGTACTGGAAATATGGGAGTTTTGGCTGGCCAAGCATCAC
8.	1041 bp - 1096 bp	ACTGAATGCAGTGGTTGACTTGCAGGACAGAAATACTGAACTGTCATATCAGCTTT
9.	1161 bp - 1211 bp	CGATCCCGATGTTCGCATTATTGAAAATCATGGCATCGAGGATGAACTGCC
10.	1286 bp - 1315 bp	CTAATGGATGGGAAAAAGATGCTAATGTTG

* GenBank accession no. AB330084

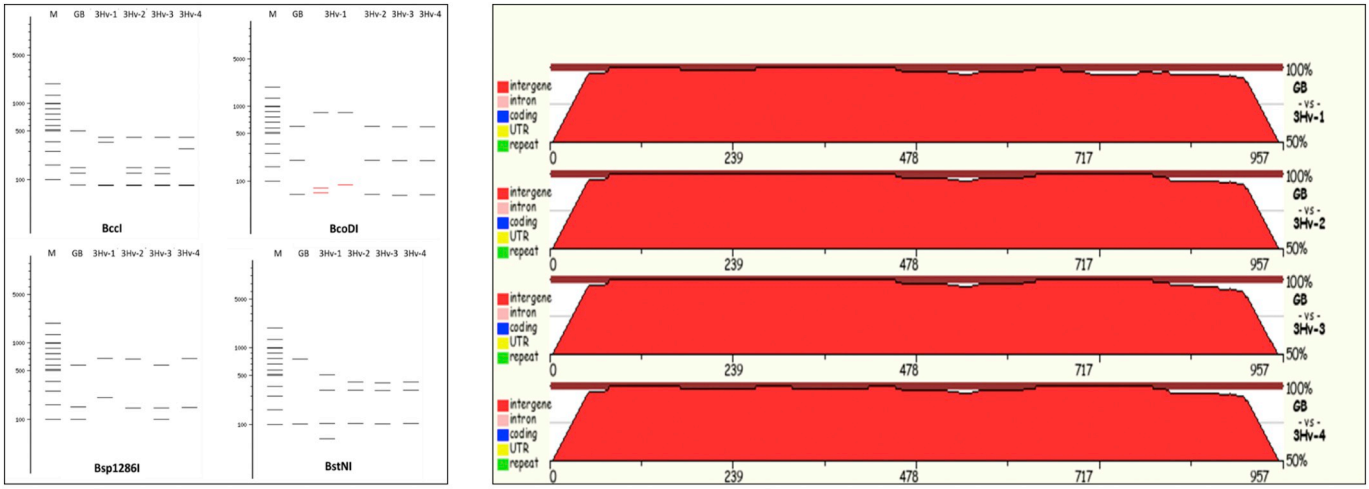

Fig. 6. (A) Restriction patterns of GB strain and 3Hv-1 to 3Hv-4 as obtained from the New England Biolabs cutting tool website (http://rebase.neb.com/rebase/rebase.html). In silico restriction endonuclease (RE) digestions were performed with *Bcc*I, *Bco*DI, *Bsp*1286I and *Bst*NI. The 100 bp molecular weight marker and 1.2% agarose gel were selected for the analysis. **(B)** Comparative genetics of GB strain and 3Hv-1 to 3Hv-4 using the zPicture pairwise alignment and visualization tool. The nucleotide sequences of the hexon HVRs of the above strains were uploaded in FASTA format on the zPicture web-site (http://zpicture.dcode.org/) for pairwise alignment using the BlastZ alignment program. The 'x' axis is the size of the nucleotide sequence in kilobases and the 'y' axis is the percent identity. The 'y' axis is set between 90% and 100%, indicating a very high level of identity. The gapless display blocks indicate homology and the intervening gap regions indicate a lack of homology.

adenovirus live vaccine was developed to prevent HAdV-4 and HAdV-7 acute respiratory infection (ARI) among the military in the United States in 1971. After providing successful protection for a prolonged period, several cases of ARI were observed among vaccinated individuals due to the emergence of mutant strains. Interestingly, analysis of vaccine strains, prototypes and field strains revealed multiple AA changes in the HVRs of hexon (Blasiole et al., 2004; Jacque et al., 2002).

In case of HAdV-3, the selection of vaccine strains is complicated due to the existence of a large number of hexon variants (Haque et al., 2018). In the present study, we have selected 3Hv-1 to 3Hv-4, as they 1) comprise 80% of all hexon variants, 2) have been circulating over longer periods when the circulation of others was shorter and 3) were co-circulating among different countries. Therefore, we have designated them as the major hexon variants. Alignment of the HVR encoding regions of 3Hv-1 to 3Hv-4 revealed 16 point mutations that resulted in 12 AA substitutions when compared to the GB strain. Among them, the lowest percentage of homology was found to be 81.81% which implied 18.19% variation in AA sequence compared to GB. 3Hv-1 to 3Hv-4 were segregated into different clusters in the phylogram because they are sufficiently different from each other and justifies their inclusion as potential candidates for vaccine development.

In this article, we have identified the conserved regions of the HVR encoding genes of 3Hv-1 to 3Hv-4 as well as other variants (3Hv-5 to 3Hv-25) of HAdV-3. From most of those regions, we have succeeded to design functional siRNAs that could be used to inhibit viral replication as there is no targeted anti-adenoviral so far. siRNAs with U, R or A satisfies functional siRNA design algorithms of Ui-Tei et al. (U) (Ui-Tei et al., 2004), Reynolds et al. (R) (Reynolds et al., 2004) and Amarzguioui et al. (A) (Amarzguioui and Prydz, 2004) respectively.

Designing siRNAs from the conserved regions to inhibit the viral replication has been used against several pathogenic viruses such as HIV, HCV, HBV, SARS coronaviruses (Hamasaki et al., 2003; Moore et al., 2005; Jacque et al., 2002). After a successful clinical trial, the siRNA-based drug (Onpatrro) is now available for the treatment of systemic disease like amyloidosis (Adams et al., 2018). Due to the presence of multiple hexon variants of HAdV-3, we have selected their conserved regions for designing siRNAs, as they will work best against all the variants. siRNA from the conserved region has been successfully used against influenza and HCV (Ge et al., 2003; Ge et al., 2004; Betáková and Svančarová, 2013; ElHefnawi et al., 2016; Tompkins et al., 2004). Hexon protein constitutes 95% of the viral capsomere (Knipe and Howley F Bernard N., 2013). If the hexon gene can be knocked down by siRNAs (Eckstein et al., 2010), the formation of complete viral particles will be prevented and without a complete capsid, HAdV will be unable to infect new host cells (Reynolds et al., 2004). We have also predicted MHC Class I epitopes from the AA sequence of the HVRs (132–450 AA) of each major hexon variant which will save time and cost of future biological work of vaccine development.

target position	target sequence 21nt target + 2nt overhang	RNA oligo sequences 21nt guide (5′→3′) 21nt passenger (5′→3′)	functional siRNA selection: Ui-Tei Reynolds Amarzguioui	seed-duplex stabilty (Tm); guide	passenger
8-30	CAGTAACTACCACCACAAACACA	UGUUUGUGGUGGUAGUUACUG GUAACUACCACCACAAACACA	U R	19.3 °C	14.3 °C
42-64	TTCCATGAAGGGAGACAATATTA	AUAUUGUCUCCCUUCAUGGAA CCAUGAAGGGAGACAAUAUUA	U R A	16.1 °C	18.1 °C
51-73	GGGAGACAATATTACTAAAGAAG	UCUUUAGUAAUAUUGUCUCCC GAGACAAUAUUACUAAAGAAG	U R A	9.8 °C	19.2 °C
52-74	GGAGACAATATTACTAAAGAAGG	UUCUUUAGUAAUAUUGUCUCC AGACAAUAUUACUAAAGAAGG	R	11.7 °C	16.1 °C
62-84	TTACTAAAGAAGGTTTGCAAATT	UUUGCAAACCUUCUUUAGUAA ACUAAAGAAGGUUUGCAAAUU	A	20.0 °C	11.7 °C
63-85	TACTAAAGAAGGTTTGCAAATTG	AUUUGCAAACCUUCUUUAGUA CUAAAGAAGGUUUGCAAAUUG	U A	20.0 °C	7.1 °C
64-86	ACTAAAGAAGGTTTGCAAATTGG	AAUUUGCAAACCUUCUUUAGU UAAAGAAGGUUUGCAAAUUGG	R	20.0 °C	10.3 °C

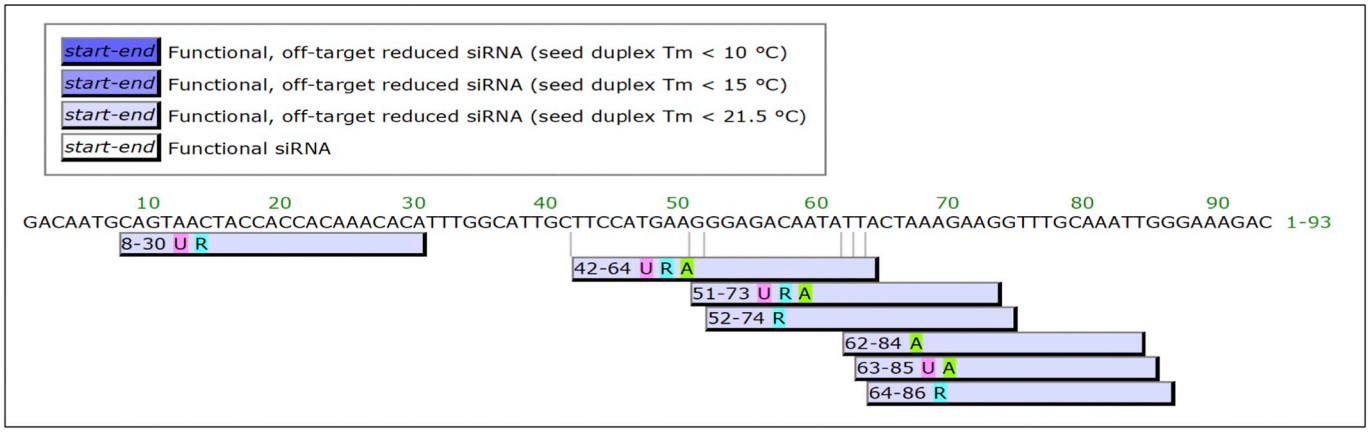

Fig. 7. The designing of siRNAs from the NT sequence of the first conserved region (GACAATGCAGTAACTACCACCACAAACACATTTGGCATTGCTTCCATGAAGG GAGACAATATTACTAAAGAAGGTTTGCAAATTGGGAAAGAC) extending from 424 to 516 bp of the hexon variants of HAdV-3 as presented in Table 3. The target positions and sequences along with the siRNA sequences and the seed-target duplex stabilities (T_m < 21.5 °C) are also shown.

Table 4
MHC class I binding epitopes as predicted from the AA sequence of the HVR of 3Hv-1 for HLA-A0101. The peptides with a % rank below 0.5 are strong binders and the peptides with a % rank between 0.5 and 2 are weak binders.

HLA	Peptide Sequence	Affinity (nM)	% Rank	Bind Level
HLA-A0101	DTDVTNEKF	603.54	0.40	Strong Binder
HLA-A0101	YTENVNLET	265.81	0.30	Strong Binder
HLA-A0101	ALAPEIVLY	3706.52	1.30	Weak Binder
HLA-A0101	ETPDSHVVY	1191.31	0.60	Weak Binder
HLA-A0101	TSDNSHANL	6941.75	2.00	Weak Binder
HLA-A0101	NTELSYQLL	2808.29	1.10	Weak Binder
HLA-A0101	LLDSLWDRT	3260.60	1.20	Weak Binder

In this study, we have found that the major hexon variants (3Hv-1 to 3Hv-4) are the most appropriate vaccine candidates against HAdV-3 and the several conserved regions located in the HVR encoding portion of the hexon gene are the suitable sites for designing siRNAs against all the hexon variants. We have designed functional siRNAs from those conserved regions and immunogenic vaccine peptide epitopes from the hexon protein. We expect that our findings could pave the way for the development of vaccine and siRNA-based therapeutics against HAdV-3 respiratory infections.

Declaration of Competing Interest

None.

Acknowledgements

A part of this project is supported by the Fundamental Research Grant Scheme (FRGS/1/2017/SKK11/AIMST/02/1) offered by the

Ministry of Higher Education, Malaysia.

Appendix A. Supplementary data

Supplementary data to this article can be found online at https://doi.org/10.1016/j.meegid.2020.104439.

References

Adams, D., Gonzalez-Duarte, A., O'Riordan, W.D., Yang, C.-C., Ueda, M., Kristen, A.V., et al., 2018. Patisiran, an RNAi therapeutic, for hereditary Transthyretin amyloidosis. N. Engl. J. Med. 379, 11–21. https://doi.org/10.1056/NEJMoa1716153.

Adhikary, A.K., 2017. Genomic diversity of human adenovirus type 3 isolated in Fukui, Japan over a 24-year period. J. Med. Microbiol. 66, 1616–1622. https://doi.org/10.1099/jmm.0.000625.

Amarzguioui, M., Prydz, H., 2004. An algorithm for selection of functional siRNA sequences. Biochem. Biophys. Res. Commun. 316, 1050–1058. https://doi.org/10.1016/j.bbrc.2004.02.157.

Betáková, T., Svančarová, P., 2013. Role and application of RNA interference in replication of influenza viruses. Acta Virol. 57, 97–104. https://doi.org/10.4149/av_2013_02_97.

Blasiole, D.A., Metzgar, D., Daum, L.T., Ryan, M.A.K., Wu, J., Wills, C., et al., 2004. Molecular analysis of adenovirus isolates from vaccinated and unvaccinated young adults. J. Clin. Microbiol. 42, 1686–1693. https://doi.org/10.1128/jcm.42.4.1686-1693.2004.

Crawford-Miksza, L., Schnurr, D.P., 1996. Analysis of 15 adenovirus hexon proteins reveals the location and structure of seven hypervariable regions containing serotype-specific residues. J. Virol. 70, 1836–1844.

Dereeper, A., Guignon, V., Blanc, G., Audic, S., Buffet, S., Chevenet, F., et al., 2008. Phylogeny.fr: robust phylogenetic analysis for the non-specialist. Nucleic Acids Res. 36, W465–W469. https://doi.org/10.1093/nar/gkn180.

Eckstein, A., Grössl, T., Geisler, A., Wang, X., Pinkert, S., Pozzuto, T., et al., 2010. Inhibition of adenovirus infections by siRNA-mediated silencing of early and late adenoviral gene functions. Antivir. Res. 88, 86–94. https://doi.org/10.1016/j.antiviral.2010.08.002.

ElHefnawi, M., Kim, T., Kamar, M.A., Min, S., Hassan, N.M., El-Ahwany, E., et al., 2016. In Silico design and experimental validation of siRNAs targeting conserved regions of multiple hepatitis C virus genotypes. PLoS One 11, e0159211. https://doi.org/10.1371/journal.pone.0159211.

Fookolaee, S.P., Karkhah, S., Saadi, M., Majumdar, S., Karkhah, A., 2019. Novel computational approaches to developing potential STAT4 silencing siRNAs for immunomodulation of atherosclerosis. Curr Comput Aided Drug Des. https://doi.org/10.2174/1573409915666191018125653.

Ge, Q., McManus, M.T., Nguyen, T., Shen, C.-H., Sharp, P.A., Eisen, H.N., et al., 2003. RNA interference of influenza virus production by directly targeting mRNA for degradation and indirectly inhibiting all viral RNA transcription. Proc. Natl. Acad. Sci. U. S. A. 100, 2718–2723. https://doi.org/10.1073/pnas.0437841100.

Ge, Q., Eisen, H.N., Chen, J., 2004. Use of siRNAs to prevent and treat influenza virus infection. Virus Res. 102, 37–42. https://doi.org/10.1016/j.virusres.2004.01.013.

Hamasaki, K., Nakao, K., Matsumoto, K., Ichikawa, T., Ishikawa, H., Eguchi, K., 2003. Short interfering RNA-directed inhibition of hepatitis B virus replication. FEBS Lett. 543, 51–54. https://doi.org/10.1016/s0014-5793(03)00400-9.

Haque, E., Banik, U., Monowar, T., Anthony, L., Adhikary, A.K., 2018. Worldwide increased prevalence of human adenovirus type 3 (HAdV-3) respiratory infections is well correlated with heterogeneous hypervariable regions (HVRs) of hexon. PLoS One 13, e0194516. https://doi.org/10.1371/journal.pone.0194516.

Jacque, J.-M., Triques, K., Stevenson, M., 2002. Modulation of HIV-1 replication by RNA interference. Nature 418, 435–438. https://doi.org/10.1038/nature00896.

Kajon, A.E., Murtagh, P., Garcia Franco, S., Freire, M.C., Weissenbacher, M.C., Zorzópulos, J., 1990. A new genome type of adenovirus 3 associated with severe lower acute respiratory infection in children. J. Med. Virol. 30, 73–76. https://doi.org/10.1002/jmv.1890300116.

Kenmoe, S., Vernet, M.-A., Le Goff, J., Penlap, V.B., Vabret, A., Njouom, R., 2018. Molecular characterization of human adenovirus associated with acute respiratory infections in Cameroon from 2011 to 2014. Virol. J. 15, 153. https://doi.org/10.1186/s12985-018-1064-x.

Kim, Y.-J., Hong, J.-Y., Lee, H.-J., Shin, S.-H., Kim, Y.-K., Inada, T., et al., 2003. Genome type analysis of adenovirus types 3 and 7 isolated during successive outbreaks of lower respiratory tract infections in children. J. Clin. Microbiol. 41, 4594–4599. https://doi.org/10.1128/jcm.41.10.4594-4599.2003.

Knipe and Howley F, Bernard, N., 2013. Fields Virology - NLM Catalog - NCBI, 6th ed. .

Lai, C.-Y., Lee, C.-J., Lu, C.-Y., Lee, P.-I., Shao, P.-L., Wu, E.-T., et al., 2013. Adenovirus serotype 3 and 7 infection with acute respiratory failure in children in Taiwan, 2010–2011. PLoS One 8, e53614. https://doi.org/10.1371/journal.pone.0053614.

Lin, G.-L., Lu, C.-Y., Chen, J.-M., Lee, P.-I., Ho, S.-Y., Weng, K.-C., et al., 2019. Molecular epidemiology and clinical features of adenovirus infection in Taiwanese children, 2014. J Microbiol Immunol Infect 52, 215–224. https://doi.org/10.1016/j.jmii.2018.07.005.

Lion, T., 2014. Adenovirus infections in immunocompetent and immunocompromised patients. Clin. Microbiol. Rev. 27, 441–462. https://doi.org/10.1128/CMR.00116-13.

Lynch, J.P., Kajon, A.E., 2016. Adenovirus: epidemiology, global spread of novel serotypes, and advances in treatment and prevention. Semin Respir Crit Care Med 37, 586–602. https://doi.org/10.1055/s-0036-1584923.

Matthes-Martin, S., Boztug, H., Lion, T., 2013. Diagnosis and treatment of adenovirus infection in immunocompromised patients. Expert Rev. Anti-Infect. Ther. 11, 1017–1028. https://doi.org/10.1586/14787210.2013.836964.

Moore, M.D., McGarvey, M.J., Russell, R.A., Cullen, B.R., McClure, M.O., 2005. Stable inhibition of hepatitis B virus proteins by small interfering RNA expressed from viral vectors. J Gene Med 7, 918–925. https://doi.org/10.1002/jgm.739.

Mysara, M., Garibaldi, J.M., Elhefnawi, M., 2011. MysiRNA-designer: a workflow for efficient siRNA design. PLoS One 6, e25642. https://doi.org/10.1371/journal.pone.0025642.

Naito, Y., Yoshimura, J., Morishita, S., Ui-Tei, K., 2009. siDirect 2.0: updated software for designing functional siRNA with reduced seed-dependent off-target effect. BMC Bioinformatics 10, 392. https://doi.org/10.1186/1471-2105-10-392.

Ovcharenko, I., Loots, G.G., Hardison, R.C., Miller, W., Stubbs, L., 2004. zPicture: dynamic alignment and visualization tool for analyzing conservation profiles. Genome Res. 14, 472–477. https://doi.org/10.1101/gr.2129504.

Pichla-Gollon SL. Structure-based Identification of a Major Neutralizing Site in an Adenovirus Hexon - PubMed n.d. https://pubmed.ncbi.nlm.nih.gov/17108028/?from_single_result=Structure-based+identification+of+a+major+neutralizing+site+in+an+adenovirus+hexon ((accessed March 19, 2020).

Reynolds, A., Leake, D., Boese, Q., Scaringe, S., Marshall, W.S., Khvorova, A., 2004. Rational siRNA design for RNA interference. Nat. Biotechnol. 22, 326–330. https://doi.org/10.1038/nbt936.

Russell, W.C., 2009. Adenoviruses: update on structure and function. J Gen Virol 90, 1–20. https://doi.org/10.1099/vir.0.003087-0.

Tompkins, S.M., Lo, C.-Y., Tumpey, T.M., Epstein, S.L., 2004. Protection against lethal influenza virus challenge by RNA interference in vivo. Proc. Natl. Acad. Sci. U. S. A. 101, 8682–8686. https://doi.org/10.1073/pnas.0402630101.

Ui-Tei, K., Naito, Y., Takahashi, F., Haraguchi, T., Ohki-Hamazaki, H., Juni, A., et al., 2004. Guidelines for the selection of highly effective siRNA sequences for mammalian and chick RNA interference. Nucleic Acids Res. 32, 936–948. https://doi.org/10.1093/nar/gkh247.

Wold, W.S.M., Tollefson, A.E., Ying, B., Spencer, J.F., Toth, K., 2019. Drug development against human adenoviruses and its advancement by Syrian hamster models. FEMS Microbiol. Rev. 43, 380–388. https://doi.org/10.1093/femsre/fuz008.

Zender, L., Hutker, S., Liedtke, C., Tillmann, H.L., Zender, S., Mundt, B., et al., 2003. Caspase 8 small interfering RNA prevents acute liver failure in mice. Proc. Natl. Acad. Sci. U. S. A. 100, 7797–7802. https://doi.org/10.1073/pnas.1330920100.

Zou, L., Zhou, J., Li, H., Wu, J., Mo, Y., Chen, Q., et al., 2012. Human adenovirus infection in children with acute respiratory tract disease in Guangzhou, China. APMIS 120, 683–688. https://doi.org/10.1111/j.1600-0463.2012.02890.x.